The majority of intestinal IgA+ and IgG+ plasmablasts in the human gut are antigen-specific

Julia Benckert,[1,2,3] Nina Schmolka,[1] Cornelia Kreschel,[1] Markus Josef Zoller,[1] Andreas Sturm,[2] Bertram Wiedenmann,[2] and Hedda Wardemann[1]

[1]Max Planck Research Group Molecular Immunology, Max Planck Institute for Infection Biology, Berlin, Germany.
[2]Department of Hepatology and Gastroenterology, Charité University Hospital Berlin, Berlin, Germany.
[3]Hepatology, Gastroenterology and Rheumatology Clinics, University Hospital Leipzig, Leipzig, Germany.

Mucosal antibody responses play a major role in mediating homeostasis with the intestinal flora. It has been suggested that imbalance in the IgA+ and IgG+ intestinal B cell repertoire may be associated with the development of diseases such as inflammatory bowel disease. Despite this, little is known about the antibody specificity of human intestinal plasmablasts. Here, we have determined the reactivity profile of single isolated IgA+ and IgG+ plasmablasts from human terminal ileum using antibody cloning and in vitro expression. We found that approximately 25% of intestinal IgA and IgG plasmablast antibodies were polyreactive; the majority were antigen-specific. Antigen specificity was not only directed against enteropathogenic microbes but also against commensal microbes and self antigens. Regardless of their reactivity, all intestinal antibodies were somatically mutated and showed signs of antigen-mediated selection, suggesting that they developed from antigen-specific B cell responses. Together, our data indicate that antigen-specific immune responses to intestinal microbes are largely responsible for the maintenance of intestinal homeostasis and thus provide a basis for understanding the deregulated immune responses observed in patients with inflammatory bowel disease.

Introduction

Constant exposure of the mucosal immune system to foreign antigens requires a tight balance between tolerance to harmless self and foreign antigens, including commensals, and the generation of protective inflammatory immune responses against invading pathogens. In humans, 80% of all antibody-secreting B cells are located in the gut mucosa (1). The vast majority of lamina propria plasmablasts produces dimeric IgA, which is constantly transported by the polymeric Ig receptor across the intestinal epithelium into the gut lumen (2). The production of secretory IgA depends on bacterial colonization of the gastrointestinal tract (3, 4). Secretory IgA plays a major role in mediating immune exclusion of luminal antigens and homeostasis with the intestinal flora as well as protection against invading pathogens (5–9). Binding of secretory IgA to intestinal foreign antigens promotes the controlled antigen sampling of microbial and food antigens by microfold cells within the epithelial layer and helps to prevent attachment of microbes to the epithelium and clearance of microbes, which have breached the epithelial barrier (10–14). Recent evidence further suggests that IgA can induce downmodulation of proinflammatory epitopes on intestinal bacteria and thereby indirectly dampens the host's immune response (15).

Although the intestinal antibody repertoire is highly dominated by IgA, 3%–4% of intestinal lamina propria B cells express IgG under physiologic conditions (1). Little is known about the development and function of intestinal IgG antibodies, but the frequency of IgG plasmablasts can be strongly increased under inflammatory conditions, e.g., in patients with inflammatory bowel disease, suggesting that imbalance in the intestinal IgA+ and IgG+ B cell repertoire may be associated with the development of disease (16–18).

Conflict of interest: The authors have declared that no conflict of interest exists.
Citation for this article: *J Clin Invest* doi:10.1172/JCI44447.

A prerequisite for understanding intestinal antibody responses is characterization of the reactivity profile of intestinal antibody secreting B cells. Surprisingly, despite the importance of humoral intestinal immune responses, little is known about the antigen specificity of intestinal IgA and IgG antibodies. Indirect evidence from mouse models suggests that nonmutated IgA antibodies with broad reactivity to self and non-self antigens as well as antigen-selected somatically mutated antibodies with specificity for individual antigens play a role in mediating homeostasis with the intestinal flora (3, 4, 7, 15, 19–21). However, the relative contribution of polyreactive versus antigen-specific intestinal plasmablasts has not been determined in mice or humans.

To examine the antibody repertoire and the specificity of human intestinal plasmablasts under steady state conditions, we cloned, expressed, and measured the reactivity of 222 recombinant monoclonal antibodies from IgA+ and IgG+ plasmablasts from terminal ileum of 3 donors. All antibodies carried high numbers of somatic mutations and showed signs of strong antigen-mediated selection. In summary, the data show that the majority of intestinal IgA+ and IgG+ plasmablasts develop from specific immune responses to self and foreign antigens, whereas about one-fourth of intestinal plasma cell antibodies are polyreactive with diverse self and nonself antigens. IgA+ and IgG+ plasmablasts with specificity for representatives of the commensal flora and for intestinal pathogens were readily identified in all donors, demonstrating that under physiologic circumstances microbial stimulation mounts strong and specific intestinal immune responses against members of the commensal flora and against intestinal pathogens.

Results

Features of intestinal human IgA and IgG plasmablast antibodies. To characterize the IgA and IgG antibody repertoire of intestinal

plasmablasts, we isolated single lamina propria IgA$^+$CD38$^+$CD27$^+$ and IgG$^+$CD38$^+$CD27$^+$ plasmablasts from terminal ileum of 3 healthy donors (HD1–HD3) and cloned their Ig heavy chain locus (*IGH*), Ig κ chain locus (*IGK*), and Ig λ chain locus (*IGL*) genes (Supplemental Figure 1 and Supplemental Tables 1–3; supplemental material available online with this article; doi:10.1172/JCI44447DS1). Intracellular FACS staining showed that nearly all IgA$^+$ intestinal plasmablasts were also surface IgA$^+$, whereas the majority of intracellular IgG$^+$ intestinal B cells lacked surface IgG expression (Supplemental Figure 1B; 80%–100% surface expression for IgA vs. 7%–25% for IgG). Dominant expression of *IGA2* in IgA$^+$ plasmablasts (70.8% ± 1.7% expression) reflects the low ratio of IgA1 to IgA2 in secretory IgA from distal parts of human gut (Figure 1A and ref. 22). IgG$^+$ plasmablasts predominantly expressed *IGG1* (51.8% ± 32.4% expression), followed by *IGG2* (35.9% ± 23.4% expression), *IGG4* (9.9% ± 8.7% expression), and *IGG3* (2.5% ± 2.3% expression) genes (Figure 1A). Independent of the isotype, all antibodies showed high numbers of somatic mutations and high ratios of replacement to silent mutations in complementarity determining region 1 (CDR1) and CDR2 compared with those in framework regions 1–3 (FWR1–FWR3) as signs of antigen-mediated selection in their *IGH* and/or *IGK* and *IGL* chain genes (Figure 1, B and C, and Supplemental Figure 3). V genes of IgA$^+$ plasmablasts carried on average 22.7 *IGH*, 13.3 *IGK*, and 13.9 *IGL* V gene mutations equivalent to nucleotide exchange rates of 7.1%, 3.6%, and 3.7%, respectively. IgG$^+$ plasmablasts carried on average 22.9 *IGH*, 15.0 *IGK*, and 13.7 *IGL* V gene mutations and thus showed mutation rates comparable to those of IgA$^+$ plasmablasts (mutation frequency: 7.6% for *IGH*, 4.0% for *IGK*, 4.4% for *IGL*; Figure 1, B and C, and Supplemental Figure 3). Clonally related antibodies with identical *IGH* V-D-J and *IGK* and *IGL* V-J rearrangements and shared somatic mutations were identified in IgA$^+$ and IgG$^+$ plasmablasts from all 3 donors (Figure 1D and Supplemental Tables 1–3). About 3.7% of all IgA antibodies (8 out of 216 antibodies) and 11.8% of all IgG antibodies (17 out of 144 antibodies) belonged to expanded clones, but clonally related B cells were not shared between the IgA$^+$ and IgG$^+$ plasmablast compartments in any of the donors (Figure 1D and Supplemental Tables 1–3). No significant differences in *IGH* gene usage and IgH CDR3 length and positive charges were observed between IgA$^+$ and IgG$^+$ plasmablasts (Figure 1E and Supplemental Figure 2A). *VH3* genes were expressed by more than 50% of IgA$^+$ plasmablasts in all donors and were also dominant in antibodies from IgG$^+$ plasmablasts. *IGK* and *IGL* light chain gene usage was also comparable, with the exception that IgA$^+$ plasmablasts showed relatively more Jκ1 and less Jκ4 usage than IgG$^+$ plasmablasts (Figure 1F and Supplemental Figure 2B).

We conclude that intestinal lamina propria IgA and IgG plasmablast antibodies show similar *Ig* gene features and undergo strong antigen-mediated clonal expansion and diversification but are not clonally related.

Polyreactive lamina propria IgA and IgG plasmablast antibodies. Polyreactive antibodies are considered to contribute substantially to the intestinal antibody repertoire and to mediate regulatory functions by immune exclusion of luminal antigens (4, 20). To determine the frequency of polyreactive intestinal antibodies, we cloned the matching *IGH*, *IGK*, and *IGL* chains genes of 137 IgA$^+$ and 85 IgG$^+$ plasmablasts into expression vectors and produced the recombinant monoclonal antibodies in vitro (23, 24). Polyreactivity was measured by ELISA with structurally different antigens, including dsDNA, LPS, and insulin (Figure 2A and refs. 23, 24). We observed interindividual variation in the frequency of polyreactive plasmablasts in both compartments, but, on average, 26% of IgA antibodies (20% for HD1, 29% for HD2, 34% for HD3) and 26% of IgG antibodies (40% for HD1, 19% for HD2, 13% for HD3) were reactive with at least 2 antigens in this assay and were thus considered polyreactive (Figure 2B and refs. 23, 24). In summary, one-fourth of human intestinal IgA$^+$ and IgG$^+$ plasmablasts from terminal ileum expressed polyreactive antibodies that showed cross-reactivity with structurally diverse self and non-self antigens.

Self-reactivity of lamina propria IgA$^+$ and IgG$^+$ plasmablasts. To test whether antibody polyreactivity was also associated with self-reactivity, we performed indirect immunofluorescence assays (IFAs) with the human epithelial cell line HEp-2, which is commonly used to detect self-reactive antibodies in serum of patients with autoimmune diseases (Figure 3, A and B, and refs. 23, 24). Antibodies that showed reactivity in this assay were categorized into anticytoplasmic, antinuclear, and antinuclear and anticytoplasmic antibodies, according to their HEp-2 subcellular staining patterns (Figure 3A). We again observed interindividual variation, but, on average, 21% of IgA$^+$ plasmablasts (10% for HD1, 29% for HD2, and 32% for HD3) and 27% of IgG$^+$ plasmablasts (26% for HD1, 19% for HD2, and 38% for HD3) expressed HEp-2 cell–reactive antibodies (Figure 3B). The majority of HEp-2–reactive antibodies recognized cytoplasmic antigens (14% of IgA, 22% of IgG), and 3% of IgA and IgG antibodies, respectively, showed nuclear and cytoplasmic staining patterns (Figure 3, B and C). True antinuclear antibody (ANA) staining patterns were observed with 4% of IgA and 1% of IgG antibodies, respectively (Figure 3, B and C). About 50% of HEp-2 binding antibodies were polyreactive (48% for IgA and 52% for IgG), and such antibodies showed predominantly cytoplasmic or nuclear and cytoplasmic staining (Figure 3C and ref. 23). Thus, self-reactivity of intestinal plasmablast antibodies is associated with polyreactivity, but antibodies with reactivity for defined HEp-2 cell self antigens, including ANAs, comprise about 7% of the intestinal IgA$^+$ and 9% of the intestinal IgG$^+$ plasmablast repertoire. To determine whether lamina propria–derived antibodies also bind to intestinal tissue self antigens that are not represented by HEp-2 cells, we tested all antibodies by IFA for reactivity with murine small intestine tissue sections (Figure 3, D–F). Hoechst staining was performed in parallel to detect cell nuclei (Figure 3D). A variety of different staining patterns against defined intestinal tissue structures and cells but also unspecific staining patterns were identified (Figure 3D). On average, 14% of IgA (10% for HD1, 16% for HD2, 19% for HD3) and 24% of IgG (29% for HD1, 26% for HD2, 13% for HD3) plasmablast antibodies showed reactivity in this assay (Figure 3E). Again polyreactive antibodies contributed to more than 50% of tissue-reactive IgA and IgG antibodies (Figure 3F). However, 3% of IgA and 6% of IgG plasmablast antibodies showed specific binding, with defined cellular or extracellular intestinal tissue structures, and were not polyreactive or self-reactive as tested by ELISA and HEp-2 cell IFA (Figure 3, C and F, data not shown, and Supplemental Tables 1–3).

In summary, 14% of intestinal IgA$^+$ and 19% of IgG$^+$ plasmablasts, respectively, expressed HEp-2 cell– or intestinal tissue–reactive antibodies. Thus, we conclude that self-reactive IgA$^+$ and IgG$^+$ plasmablasts are part of the normal intestinal plasmablast compartment, including cells that express antibodies with specificity for nuclear and intestinal tissue antigens.

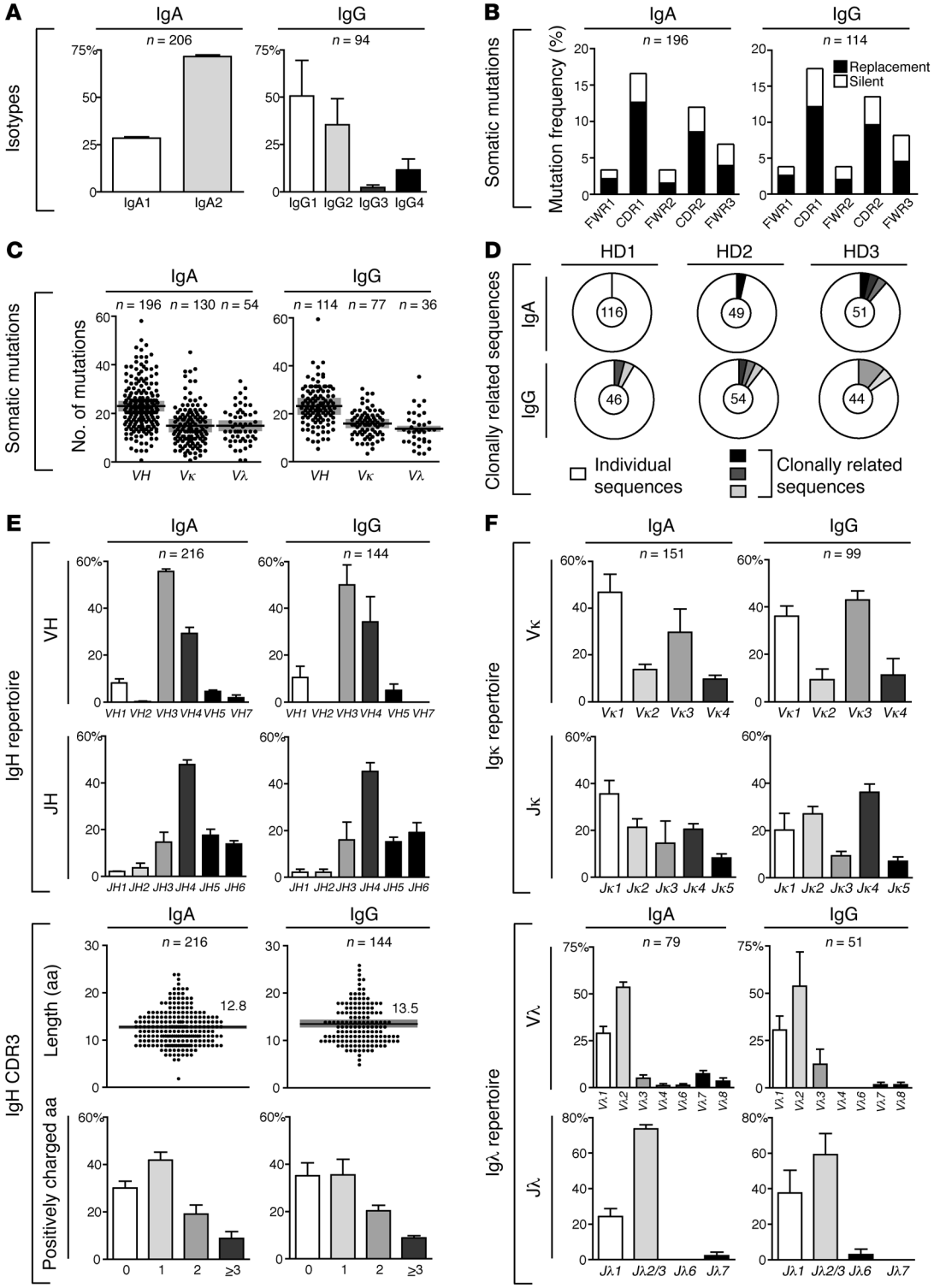

Figure 1

Ig gene analysis of intestinal IgA+ and IgG+ plasmablasts. The *IGH* gene sequences of IgA+ and IgG+ plasmablasts from the terminal ileum of HD1–HD3 were analyzed for (**A**) isotype subclass usage, (**B**) frequency of replacement (black) and silent (white) mutations in FWRs and CDRs, (**C**) absolute number of somatic mutations in V genes, (**D**) clonal relationships, (**E**) *IGH* V family and J gene usage and IgH CDR3 aa length and positive charges, and (**F**) *IGK* and *IGL* V family and J gene usage. The absolute number of sequences analyzed is indicated over each graph. Error bars in bar graphs indicate standard deviation of means for individual patients. Average means of IgH CDR3 length and of V gene somatic mutations are indicated by horizontal lines in the respective graphs. Gray bars indicate standard deviation of means of individual donors (each donor is indicated by an individual symbol). The number of tested antibodies is indicated in the pie chart center. Shaded areas in pie charts indicate clonally related sequences. *P* values were calculated to compare data from IgA and IgG plasmablasts but did not reach values below 0.05 and thus are not indicated.

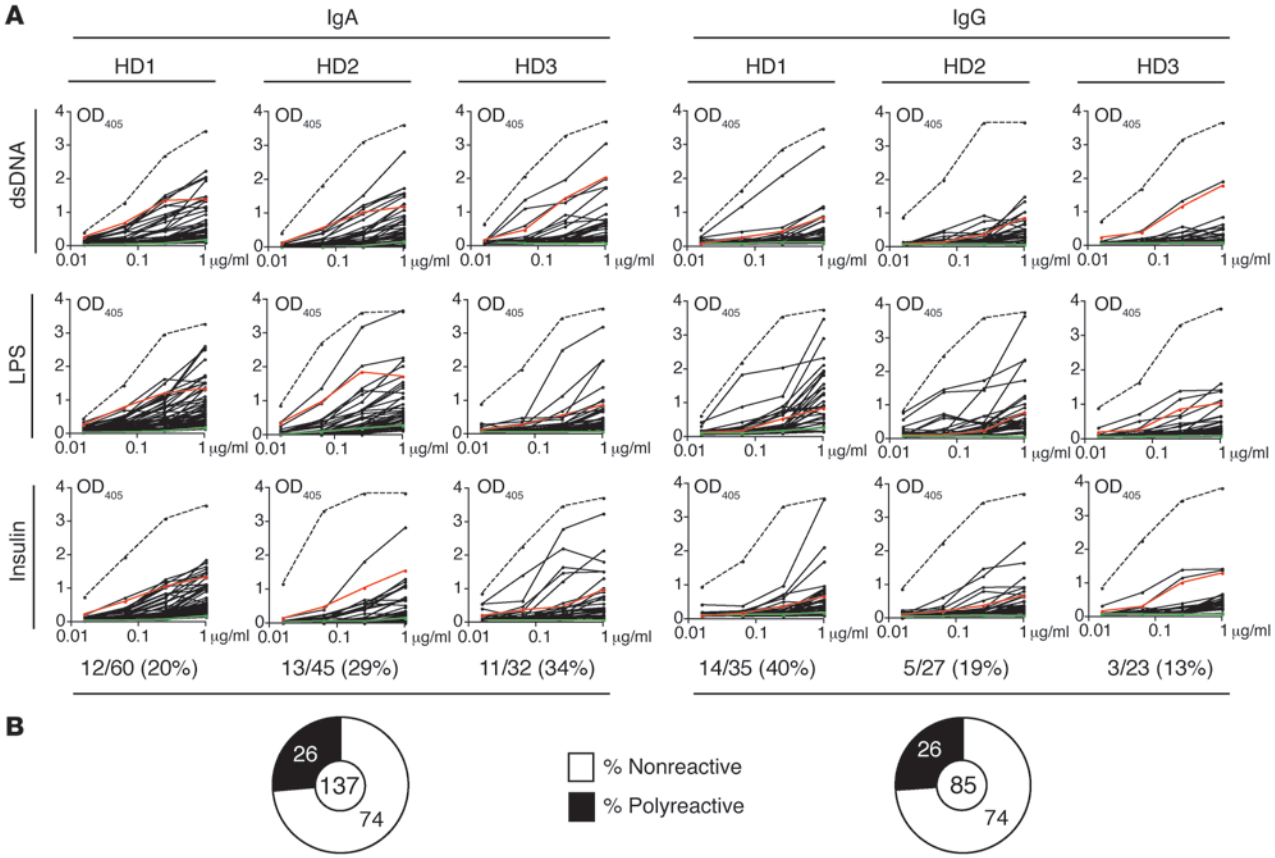

Figure 2

Polyreactivity of intestinal IgA and IgG plasmablast antibodies. IgA and IgG plasma cell antibodies from HD1–HD3 (solid lines) were tested for polyreactivity with dsDNA, ssDNA, insulin, and LPS by ELISA in at least 3 independent experiments. (**A**) Representative graphs for dsDNA, LPS, and insulin are shown. Dotted lines represent the high positive control antibody ED38 (40). Red and green lines show the low positive control antibody JB40 and the negative control antibody mGO53, respectively (23). The number and frequency of polyreactive antibodies with reactivity to at least 2 structurally different antigens out of all tested IgA and IgG antibodies is indicated below the respective graphs for each donor (23, 24). (**B**) Pie charts summarize the frequency of nonpolyreactive (white) and polyreactive (black) antibodies out of all tested IgA and IgG antibodies from all donors as measured in 3 independent experiments. The number of tested antibodies is indicated in the pie chart center. Other numbers in pie charts represent the frequency of polyreactive and nonpolyreactive antibodies, respectively.

Reactivity of lamina propria IgA and IgG plasmablast antibodies with commensal and pathogenic microorganisms. Exposure to commensal and pathogenic microorganisms can induce antigen-specific intestinal B cell responses. To identify IgA and IgG antibodies from lamina propria plasmablasts that show reactivity with specific intestinal microorganisms, using whole cell ELISA, we tested all 222 antibodies for binding to a panel of representative commensal bacteria: *E. coli*, *Enterobacter cloacae*, *Enterococcus faecalis*, *Morganella morganii*, *Bacteroides thetaiotaomicron*, the probiotic strains *E. coli* Nissle 1917 and *Lactobacillus reuteri*, and the enteropathogenic bacterium *Salmonella typhimurium* (Figure 4, Supplemental Tables 1–3, and data not shown). In addition, all antibodies were tested for ELISA binding to virus-like particles (VLPs) of enteritis-causing rotavirus (Figure 4 and Supplemental Tables 1–3).

On average 7% of IgA antibodies and 6% of IgG antibodies showed low levels of cross-reactivity with several bacterial species but were not reactive with dsDNA, LPS, and insulin and were thus considered bacteria polyreactive (Figure 4, A and B, and Supplemental Tables 1–3). In contrast, 4 IgA and 7 IgG antibodies from all 3 donors showed high reactivity with individual microbes or rotavirus in the ELISAs (Figure 4C and Supplemental Tables 1–3). Four antibodies were highly reactive with *E. coli* (HD2g36, HD3g76, HD3g144λ, HD3g149λ), 2 recognized *E. cloacae* (HD1a57, HD3a55) and *M. morganii* (HD3g71, HD3a159), respectively, and 3 showed specificity to rotavirus (HD2a53, HD3g26, HD3g94). FACS analysis confirmed that the antibodies HD3g76, HD3g144λ, and HD3g71 reacted specifically with *E. coli* and *M. morganii*, respectively (Figure 4D). By Western blotting, we could identify LPS as specific target antigen of 2 *E. coli*–reactive antibodies (Supplemental Figure 4). Surprisingly, none of the antibodies with specificity for the same microbe that were cloned from B cells of the same individual were clonally related (Supplemental Tables 1–3). Specificity for *E. coli* was limited to IgG antibodies, whereas anti–*E. cloacae* antibodies were IgAs, and *M. morganii* and rotavirus-reactive antibodies, respectively, were cloned from IgA^+ and IgG^+ plasmablasts (Figure 4C and Supplemental Figure 4). Specific antibodies against *E. faecalis*, *S. typhimurium*, *B. thetaiotaomicron*, *E. coli* Nissle, and *L. reuteri* were not identified (Supplemental Tables 1–3 and data not shown).

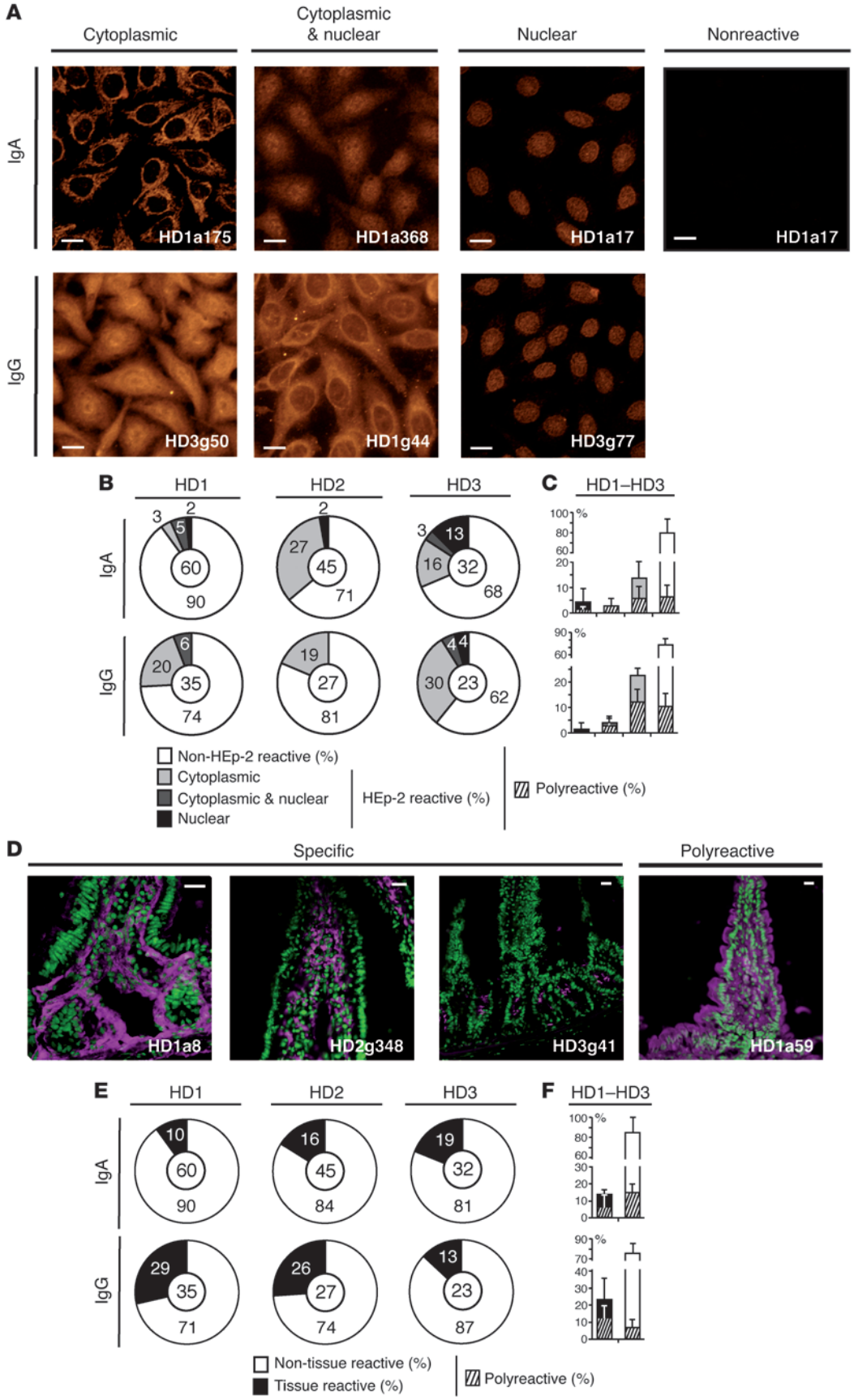
A
Cytoplasmic
Cytoplasmic & nuclear
Nuclear
Nonreactive
IgA
IgG
HD1a175
HD1a368
HD1a17
HD1a17
HD3g50
HD1g44
HD3g77
B
HD1
HD2
HD3
C
HD1–HD3
Non-HEp-2 reactive (%)
Cytoplasmic
Cytoplasmic & nuclear
Nuclear
HEp-2 reactive (%)
Polyreactive (%)
D
Specific
Polyreactive
HD1a8
HD2g348
HD3g41
HD1a59
E
F
Non-tissue reactive (%)
Tissue reactive (%)
Polyreactive (%)

Figure 3

Self-reactivity of IgA and IgG lamina propria plasmablasts. IgA and IgG plasma cell antibodies from HD1–HD3 were tested for self-reactivity (**A**–**C**) by IFA with HEp-2 cells and (**D**–**F**) on intestinal tissue sections. (**A**) Representative cytoplasmic, cytoplasmic and nuclear, and nuclear HEp-2 cell staining patterns. A non-HEp-2 cell–reactive antibody is shown for comparison. Scale bars: 20 μm. (**B**) Pie charts summarize the frequency of non-HEp-2 cell–reactive (white) and HEp-2 cell–reactive antibodies, with cytoplasmic (light gray), cytoplasmic and nuclear (dark gray), and nuclear (black) reactivity. The number of tested antibodies is indicated in the pie chart center. Other numbers in each section represent the frequency of antibodies for each condition, respectively. (**C**) Bar graphs summarize the frequency of antinuclear (black), anticytoplasmic and antinuclear (dark gray), anticytoplasmic (light gray), and non-self-reactive (white) antibodies for HD1–HD3. Shaded areas indicate polyreactive antibodies. Standard deviation of means is indicated. (**D**) Representative specific and polyreactive intestinal tissue staining patterns (purple). Hoechst-stained nuclei are shown in green. Scale bars: 50 μm. (**E**) Pie charts show the frequency of non-intestinal tissue–reactive antibodies (white) and intestinal tissue–reactive antibodies (black) for each HD. The number of tested antibodies is indicated in the pie chart center. Other numbers in each section represent the frequency of antibodies for each condition, respectively. (**F**) Bar graphs summarize the frequency of tissue reactive (black) and non-tissue reactive (white) IgA and IgG antibodies, respectively, for HD1–HD3. Shaded areas indicate polyreactive antibodies. Standard deviation of means is indicated.

We concluded that, despite the enormous diversity of the intestinal flora, individual members of the commensal flora and intestinal pathogens elicit strong intestinal IgA and IgG plasmablast responses.

Antibody reactivity profile of the intestinal IgA⁺ and IgG⁺ plasmablast repertoire. Overall, IgA⁺ and IgG⁺ plasmablasts in lamina propria of the terminal ileum showed similar reactivity profiles (Figure 5). On average, 26% of IgA and of IgG antibodies were polyreactive with diverse self and foreign antigens, including bacteria. Cross-reactivity with diverse bacterial strains in the absence of broad levels of polyreactivity was observed for 7% of IgA and 5% of IgG antibodies. We conclude that in total about one-third of IgA⁺ and IgG⁺ lamina propria plasmablast antibodies are polyreactive or cross-reactive with bacteria, whereas the majority of intestinal plasmablasts (66% of IgA⁺ and 70% of IgG⁺ cells) express nonpolyreactive and non-cross-reactive antibodies, including self-reactive antibodies that react with nuclear or intestinal tissue antigens and antibodies specific for common intestinal microbes and pathogens.

In summary, the data suggest that the majority of intestinal IgA and IgG plasmablast antibodies are generated in a specific response to antigenic stimulation and do not show unspecific binding to intestinal microbes or are polyreactive with diverse self and foreign antigens.

Discussion

Although the vast majority of human antibody-producing B cells is located in the gut, surprisingly little is known about the *Ig* gene repertoire in this compartment as compared with systemic B cell populations (25). Most analyses of intestinal plasmablast antibodies were based on amplification of selected *VH* genes from bulk-sorted IgA⁺ B cells and thus could not provide detailed information about *IGH*, *IGK*, and *IGL* chain gene usage or antibody reactivity (26–28). The *IGH*, *IGK*, and *IGL* chain gene repertoire of intestinal plasmablasts showed no significant differences to systemic B cell populations, including IgG⁺ peripheral blood memory B cells. Our results confirm the high *Ig* gene mutation load and strong clonal expansion of IgA⁺ plasmablasts in terminal ileum and report similar results for IgG⁺ plasmablasts (27, 28). Clonally related antibodies were identified in IgA⁺ and IgG⁺ plasmablasts but were not shared between both compartments, suggesting that they may originate from independent precursor cells. However given the relatively small number of sequences that can be analyzed by recombinant antibody production, definite answers to the question of whether or not there is clonal overlap between the 2 compartments will require deeper sampling, especially of the IgG⁺ population, e.g., using next-generation sequencing.

Dominant expression of IgA2, with higher resistance to bacterial proteases than IgA1, has been reported in the terminal ileum and is associated with higher bacterial load in more distal parts of the intestine (1, 22). High amounts of TI bacterial carbohydrate antigens present in the gut may further support class switching to IgG2 and IgG4 as compared with systemic B cell compartments or IgG plasmablasts in the proximal small intestine with lower bacterial load (29). The low inflammatory potential of IgG2 and IgG4, with limited ability to mediate complement fixation and low affinity for activating IgG Fcγ receptors, may play an important role in regulating intestinal immune responses and thus in maintaining tolerance to the intestinal microflora (1).

Similar to the *Ig* gene repertoire of peripheral antigen-experienced B cells, the antibody response of intestinal plasmablasts was dominated by VH3 family members followed by *VH4* and *VH1* genes (30–32). Differences in *Ig* gene usage between IgA⁺ and IgG⁺ plasmablasts were limited to an increased Jκ1 usage in IgA⁺ plasmablasts, suggesting that many *IGK* light chain genes in this compartment originate from successful primary *Ig* gene rearrangements.

The diversity of the *Ig* gene repertoire precludes the prediction of antibody reactivity based on sequence analysis alone, particularly for cells expressing somatically mutated *Ig* genes. Whereas the antibody reactivity of murine and human peripheral blood and tissue B cells has been studied extensively in stable cell lines and by antibody cloning, the reactivity of intestinal antibodies has not been analyzed on a cellular level. Secretory IgA antibodies show reactivity with commensal bacteria and play a role in protection against commensal and pathogenic intestinal microbes, but these experiments were unable to address whether mucosal IgA responses are dominated by polyreactive or antigen-specific antibodies (7, 20, 33, 34). About one-fourth of IgA and IgG plasma cell antibodies showed polyreactivity with diverse self and non-self antigens. Polyreactivity is a typical feature of natural antibodies, but somatic mutations can contribute strongly to polyreactivity of circulating IgG⁺ memory B cells in humans, which show frequencies of polyreactive antibodies similar to those of intestinal plasmablasts (32). Thus, antibody polyreactivity of intestinal plasmablasts is unlikely a germline encoded feature and may be acquired by somatic mutations. The finding that a sizable fraction of IgA⁺ and IgG⁺ intestinal plasmablasts from nonautoimmune donors express self-reactive antibodies with specificity for systemic cellular or tissue-specific antigens supports the idea that polyreactivity and self-reactivity is a by-product of somatic mutations, as observed for peripheral IgG memory B cell antibodies (32). Not mutually exclusive, selection of somatically mutated variants of polyreactive naive antibodies may help to narrow the antigen specificity and may thus contribute to antigen-specific immune responses against foreign antigens (35). Indeed, we identified individual antibodies with high reactivity to

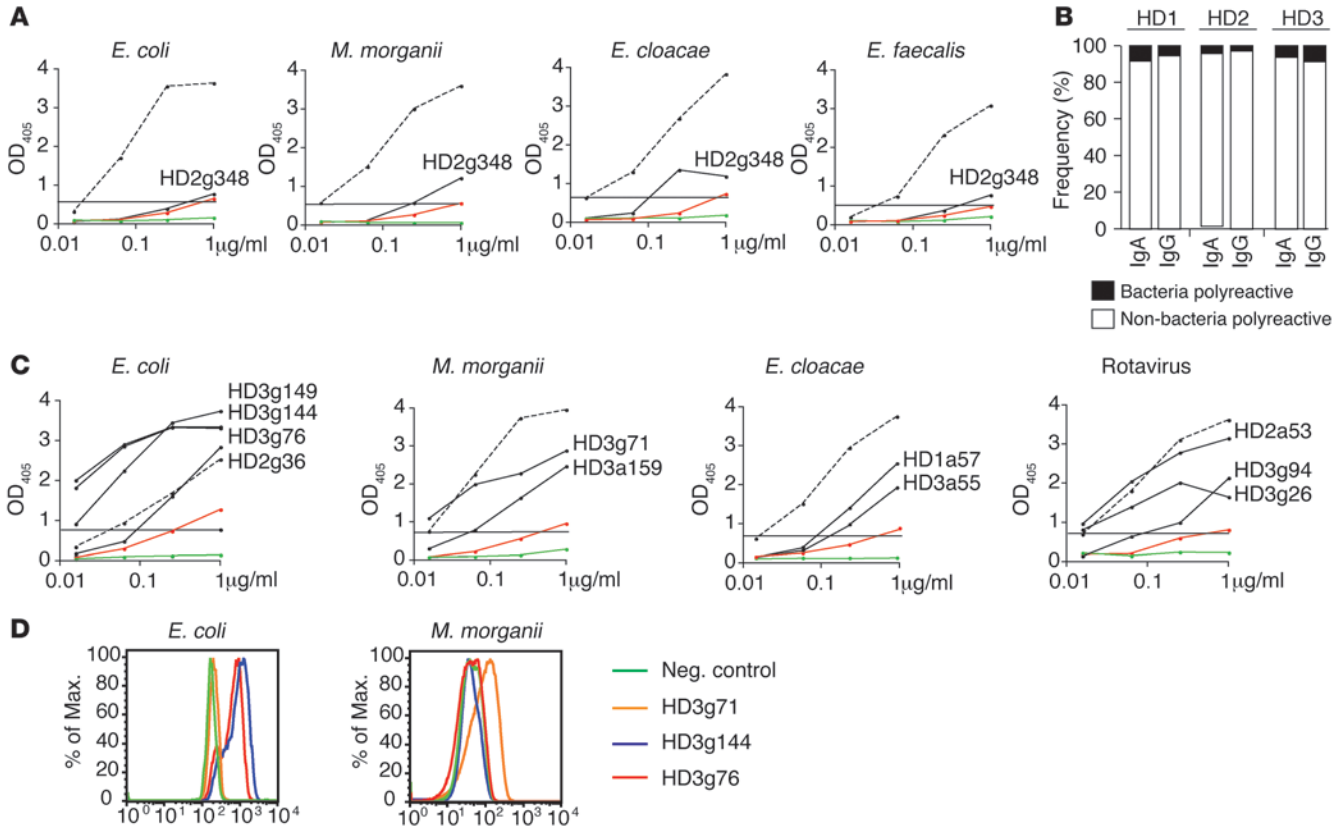

Figure 4

Reactivity of IgA and IgG lamina propria plasmablast antibodies with intestinal microbes. IgA and IgG plasma cell antibodies from HD1–HD3 were tested for reactivity with a panel of nonpathogenic and enteropathogenic intestinal microbes. The data shown are representative for at least 2 independent experiments. (**A**) ELISA graphs show the reactivity profile (black line) of a representative bacteria-polyreactive antibody (HD2g348) with *E. coli*, *M. morganii*, *E. cloacae*, and *E. faecalis*. High positive (dashed line, ED38; ref. 40), low positive (red line, JB40; ref. 23), and nonreactive (green line, mGO53; ref. 23) antibodies were included in each assay for comparison. Horizontal lines indicate the cutoff OD_{405} in each assay. (**B**) Bar graphs summarize the frequency of bacteria polyreactive antibodies (black) and non-bacteria polyreactive IgA and IgG antibodies (white) in each donor as determined by ELISA as in **A**. (**C**) Representative ELISA graphs show the reactivity of *E. coli*, *M. morganii*, *E. cloacae*, and rotavirus-specific IgA and IgG plasma cell antibodies from HD1–HD3. Clone names of bacteria-specific antibodies are indicated in the graphs. Additional high positive (dashed line, ED38; ref. 40), low positive (red line, JB40; ref. 23) and nonreactive (green line, mGO53; ref. 23) control antibodies were included in each assay for comparison. Horizontal lines indicate the cutoff OD_{405} in each assay. (**D**) Histograms show binding of *E. coli*–specific (HD3g76, HD3g144) and *M. morganii*–specific (HD3g71) antibodies to whole bacteria as measured by FACS. Secondary antibody only (neg. control) was included as control in all assays.

specific commensal bacteria strains or intestinal tissue structures and low levels of cross-reactivity with other foreign or self antigens. Antibody cross-reactivity has also been reported for somatically mutated antibodies with high affinity for defined self and non-self antigens, including DNA and HIV surface glycoproteins, and may contribute to increased antigen-binding (36–38).

The majority of intestinal IgA^+ and IgG^+ plasmablasts lacked polyreactivity with self and non-self antigens, and only a small fraction showed low levels of polyreactivity with intestinal bacteria. Surprisingly, despite the enormous diversity of the intestinal microbiota, we were able to identify IgA and IgG antibodies with specificity for members of the commensal flora and for enteropathogenic rotavirus in all donors, suggesting that microbial challenge can mount strong immune responses by the intestinal immune system. Studies in mice associated with only 1 intestinal bacterial species have shown that a fraction of intestinal IgA antibodies show specificity for the associated strain (3, 19). Our results suggest that specific B cells against individual intestinal microbes and microbial surface antigens, such as LPS from commensal *E. coli*, are also generated under physiologic circumstances in humans, with a diverse flora of an estimated 1,000–1,500 different species (39). Substantially deeper sampling of the intestinal antibody repertoire will be required to determine whether differences in the antibody response to specific members of the commensal microflora can be observed.

Naturally, we were unable to identify the cognate antigens for all intestinal antibodies, but we did not observe any significant differences in the reactivity of IgA and IgG antibodies. Thus, although sequence analysis showed that intestinal IgA^+ and IgG^+ plasmablasts are not clonally related and therefore do not originate from common precursors, they may be generated in response to the same antigenic stimulus. Thus, lack of efficient transport into the gut lumen rather than differences in the antibody reactivity profile may account for differences in the effector functions of intestinal IgA and IgG antibodies (1).

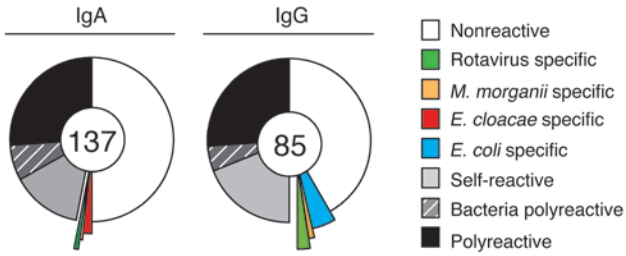

Figure 5
Antibody reactivity of human IgA+ and IgG+ lamina propria plasmablasts. Pie charts summarize the frequency of IgA+ and IgG+ plasmablasts of unknown specificity (white), of plasmablasts with specificity for intestinal microbes (blue, *E. coli*; yellow, *M. morganii*; red, *E. cloacae*; green, rotavirus) or self antigens (light gray, HEp-2 or intestinal tissue), and of unspecific bacteria-reactive (hatched dark gray) and polyreactive (black) plasmablasts as percentages of all tested IgA and IgG antibodies, respectively, from HD1–HD3. The number of tested antibodies is indicated in the pie chart centers.

In summary, the data shown here demonstrate that the intestinal IgA+ and IgG+ plasmablast repertoire in humans is similar in its *Ig* gene features and reactivity profile. The majority of intestinal IgA+ and IgG+ plasmablasts express antigen-specific antibodies, which are generated in response to commensal and enteropathogenic microbes. The data provide the baseline for further studies on changes in the intestinal antibody repertoire under chronic inflammatory conditions. Defining the reactivity of intestinal antibodies in the presence of a normal flora is essential to understand how homeostasis with the intestinal flora is maintained under physiologic circumstances and deregulated in disease.

Methods

Tissue samples. Surgical samples from unaffected terminal ileum of 3 donors undergoing right-sided hemicolectomy, due to malignancy of ascending colon (HD1, male, 64 years old; HD2, female, 73 years old) or cecum (HD3, male, 63 years old), were obtained after signed informed consent in accordance with institutional review board–reviewed and –approved protocols at the Charité University Hospital, Berlin. None of the donors had a history of intestinal inflammation, and the samples showed no signs of inflammation as determined by macroscopic evaluation and histopathologic examination of the adjacent mucosa. All donors showed normal blood counts, as measured by routine laboratory diagnostics, and had not received any immunosuppressive or immunomodulatory treatment.

FACS analysis and single B cell sorting. Tissue samples weighed between 1.1 and 1.6 g. Lamina mucosa and propria were dissected from lamina muscularis propria by blunt preparation and cut into 2- to 3-mm pieces. Digestion of tissue pieces was performed by 0.1% DNase and 0.1% collagenase in PBS at 37°C under constant stirring for 60 minutes. Lamina propria lymphocytes were purified and separated from epithelial cells and debris by discontinuous Ficoll density gradient centrifugation (GE Healthcare). Purified lamina propria lymphocytes were stained on ice with fluorochrome-coupled anti-human CD38 fluorescein isothiocyanate (BD Bioscience Pharmingen), anti-human CD27 PE (BD Bioscience Pharmingen), anti-human CD19 PE and cyanine dye Cy7 (BD Bioscience Pharmingen), anti-human IgG allophycocyanin (APC; BD Bioscience Pharmingen), or anti-human IgA APC (Jackson ImmunoResearch Laboratories Inc.). Intracellular stainings were performed after fixation with 1% PFA for 30 minutes and permeabilization with 0.1% saponin for 20 minutes. Single CD38+CD27+IgA+ or CD38+CD27+IgG+ plasmablasts were sorted into 96-well PCR plates (Eppendorf) containing 4 μl lysis solution (0.5x PBS containing 10 mM DTT and 8 U RNAsin [Promega]), using a FACSVantage cell sorter with Diva configuration (Becton Dickinson). PCR plates were immediately frozen on dry ice and stored at –80°C until further processing, as previously described (23, 24).

PCR amplification and expression-vector cloning. Single cell cDNA synthesis was performed in the 96-well sort plates using 150 ng random hexamer primer [pd(N)6, GE Healthcare], 0.5 μl dNTP mix with 10 mM of each nucleotide (Invitrogen), 1 μl 0.1 mM DTT, 0.5% v/v NP40, 10 U RNase Inhibitor (RNAsin, Promega), and 50 U SuperScript III (Invitrogen) at 50°C (23, 24). *IGG* or *IGA* heavy chain genes and *IGK* or *IGL* light chain genes were amplified in 2 rounds of nested PCR. Each round of PCR was performed for 50 cycles at 94°C for 30 seconds, 57°C (*IGH* and *IGK*) or 60°C (*IGL*) for 30 seconds, and 72°C for 55 seconds (first PCR) or 45 seconds (second PCR) (23, 24). Primer nucleotide sequences were as previously described (24). Reverse primers for *IGA* were 3′CaCH1 (nucleotide sequence: TGGGAAGTTTCTGGCGGTCACG) for the first PCR and 3′CaCH1-2 as nested internal primer for the second PCR (nucleotide sequence: GTCCGCTTTCGCTCCAGGTCACACT), respectively. PCR amplification efficiency for amplification of matching *IGH* and *IGL* chain genes was between 30%–45% (24). All PCR products were sequenced after purification (Qiaquick, Qiagen) and analyzed for *Ig* gene usage, CDR3 features, number of V gene mutations, and isotype subclass by IgBLAST (http://www.ncbi.nlm.nih.gov/igblast/; Supplemental Tables 1–3 and refs. 23, 24). Second PCR products for *IGL* genes contained restriction sites allowing direct cloning into expression vectors (24). For *IGG*, *IGA*, and *IGK*, genes restriction sites for expression vector cloning were introduced after sequencing using gene-specific V and J gene primers and first PCR products as a template. In about 80%–85% of cases, PCR products were successfully cloned on the first attempt. All *IGH*, *IGK*, and *IGL* chain genes were sequenced after cloning to confirm identity with the original PCR products.

Ig gene sequence analysis. Sequence analysis was performed as described previously (24). In brief, sequences were analyzed by IgBLAST comparison with GenBank (http://www.ncbi.nlm.nih.gov/igblast/) to identify germline V(D)J gene segments with the highest homology. Polymorphisms were identified by comparison with published germline sequences (IgBLAST, http://www.ncbi.nlm.nih.gov/igblast/ and ImMunoGeneTics information system, http://imgt.cines.fr). Shared V gene segment mutations in *Ig* genes with different V(D)J rearrangements amplified from B cells of the same donor would be considered as polymorphic alleles that are not included in public databases but were not observed. Clonal relationships were identified based on identical *IGH* and *IGL* chain gene rearrangements with shared V gene segment mutations in B cells from the same individual. IgH CDR3 length was determined as indicated in IgBLAST, by counting the aa residues following FWR3 up to the conserved tryptophan-glycine motif in all JH segments or up to the conserved phenylalanine-glycine motif in JK and JL segments (40). The number of positively charged (histidine, arginine, lysine) aa was determined for each IgH CDR3 region. Numbers of V gene somatic mutations were counted for FWR1–FWR3 inclusively. Frequencies of replacement and silent mutations in FWR1–FWR3 and CDR1 and CDR2 were calculated for each *IGH*, *IGK*, and *IGL* chain gene. Ratios of replacement to silent mutations in FWR1–FWR3 and CDR1 and CDR2 were calculated based on the total number of *IGH*, *IGK*, and *IGL* chain gene nucleotides analyzed.

Antibody production and purification. Human embryonic kidney 293T cells (ATCC, no. CRL-11268) were cultured in 150-mm plates (Falcon, Becton Dickinson) under standard conditions in DMEM (GibcoBRL) supplemented with 10% heat-inactivated ultralow IgG FCS (Invitrogen), 1 mM sodium pyruvate (GibcoBRL), 100 μg/ml streptomycin (GibcoBRL), 100 U/ml penicillin G (GibcoBRL), and 0.25 μg amphotericin (GibcoBRL). Transient transfections were performed at 80% cell confluency with equal amounts

(10–15 μg each) of IgH and corresponding IgL chain encoding plasmid DNA as described previously (23, 24). The cells were cultured for 6 days in 25 ml DMEM supplemented with 1% Nutridoma-SP (Roche) before supernatants were harvested and analyzed by ELISA for recombinant antibody production. Successful antibody production, as determined by IgG1 concentrations above 5 μg/ml in culture supernatants, was observed in over 80% of cases. Antibodies were purified with protein G beads (GE Healthcare) according to manufacturer's instructions.

ELISA and indirect IFA. Antibodies were tested for polyreactivity with dsDNA, single-stranded DNA (ssDNA), LPS, and insulin by ELISA as described previously (23, 24). In brief, ELISA plates (Costar) were coated with 5 μg/ml human recombinant insulin or 10 μg/ml dsDNA, ssDNA, or LPS (all from Sigma-Aldrich) in PBS, respectively, overnight. Plates were incubated with 50 μl nonpurified or purified antibody at 1 μg/ml and 3 consecutive 1:4 dilutions in PBS. Recombinant human monoclonal antibodies mGO53 (nonpolyreactive; ref. 23), JB40 (low polyreactive; ref. 23), and ED38 (highly polyreactive; ref. 41) served as controls and were included on each plate. Bound antibodies were detected using HRP-coupled goat anti-human IgG (Jackson ImmunoResearch Laboratories Inc.) at a concentration of 0.8 μg/ml in PBS with 2 mM EDTA and 0.05% Tween-20 and HRP chromogenic substrate (ABTS; Pierce) according to the manufacturer's instructions. ODs were measured at 405 nm, and antibody binding was determined using Soft-Max software (Molecular Devices). ELISAs against bacteria and VLPs of rotavirus (VLP; ref. 42) were performed as follows: *E. coli* (isolated from human stool), *E. coli* Nissle 1917 (Ardeypharm), *E. faecalis* (Deutsche Sammlung von Mikroorganismen und Zellkulturen [DSMZ] 20478), *E. cloacae* (DSMZ 30054), *S. typhimurium* (DSMZ 4224), *M. morganii* (DSMZ 6675), *L. reuteri* (DSMZ 20053), and *B. thetaiotaomicron* (DSMZ 2079) were grown as single colony culture under appropriate conditions to an OD_{600} of 1.0–2.0. Bacteria were fixed for 20 minutes in 0.2% PFA. ELISA plates were pretreated with 100 μl Poly-L-Lysine (0.001% w/v, Sigma-Aldrich P8920) for 30 minutes, washed, and then coated with 50 μl of 1×10^7/ml bacteria suspension in PBS overnight. VLPs were coated to ELISA plates at 1 μg/ml. Plates were centrifuged at 1,811 *g* for 15 minutes, and ELISAs were performed as described above.

Hep-2 IFA was performed as previously described (23, 24). In brief, HEp-2 cell–coated slides (Bion Enterprises LTD) were incubated in a moist chamber at ambient temperature with 20 μl purified antibodies at 100 μg/ml for 30 minutes, washed in PBS, and incubated for 30 minutes with Cy3-labeled goat anti-human Ig (Jackson ImmunoResearch Laboratories Inc.) according to the manufacturer's instructions. Control stainings with PBS and ANA-negative and ANA-positive control sera (INOVA Diagnostics) were performed in all experiments.

Murine intestinal tissue sections were prepared from C57BL/6 mice. The small intestine was removed, washed in ice-cold PBS, and incubated in 4% PFA for 20 minutes at 4°C. The tissue was washed again and incubated in 0.5 M sucrose-PBS solution until it sank to the ground. Incubation in 1 M sucrose PBS solution overnight followed. Tissue samples were embedded in cryo-medium and stored at –80°C until further use. IFA was performed using 6-μm transverse sections as described for HEP-2 cells.

LPS extraction and Western blotting. LPS was extracted from *E. coli* using a commercially available LPS Extraction Kit (Intron Biotechnology), separated on a 10%–20% Tris-Tricine gel (Bio-Rad), and transferred onto nitrocellulose. Membranes were blocked in PBS with 0.05% Tween20 and 5% skim milk powder overnight at 4°C and incubated with the test antibody (1 μg/ml) for 1 hour. Bound antibodies were detected using horseradish peroxidase–labeled anti-human IgG and Western Lightning Plus-ECL (PerkinElmer) as substrate.

Statistics. *P* values for *Ig* gene repertoire analysis, analysis of positive charges in IgH CDR3, and antibody reactivity were calculated by Fisher Exact test or χ^2 test. *P* values for IgH CDR3 length and V gene mutations were calculated by nonpaired 2-tailed Student's *t* test. *P* values below 0.05 were considered significant.

Acknowledgments

We thank Christian Busse for help with sequence analysis; Toralf Kaiser for assistance with single cell sorting; Didier Poncet and Annie Charpilienne for reagents; Juanita Angel, Catherine Chaput, Thomas Berg, and all members of the laboratory for help and discussion; and Marc Ehlers for critical reading of the manuscript. J. Benckert was supported by the German Research Foundation (BE3988). H. Wardemann received funding from the Behrens Weise Foundation. M.J. Zoller was supported by the IMPRS-IDI, Berlin.

Received for publication July 21, 2010, and accepted in revised form January 26, 2011.

Address correspondence to: Hedda Wardemann, Max Planck Research Group Molecular Immunology, Max Planck Institute for Infection Biology, 10117 Berlin, Germany. Phone: 49.0.30.28460.360; Fax: 49.0.30.28460.363; E-mail: wardemann@mpiib-berlin.mpg.de.

1. Brandtzaeg P, Johansen FE. Mucosal B cells: phenotypic characteristics, transcriptional regulation, and homing properties. *Immunol Rev*. 2005; 206:32–63.
2. Brandtzaeg P, Prydz H. Direct evidence for an integrated function of J chain and secretory component in epithelial transport of immunoglobulins. *Nature*. 1984;311(5981):71–73.
3. Shroff KE, Cebra JJ. Development of mucosal humoral immune responses in germ-free (GF) mice. *Adv Exp Med Biol*. 1995;371A:441–446.
4. Macpherson AJ, Gatto D, Sainsbury E, Harriman GR, Hengartner H, Zinkernagel RM. A primitive T cell-independent mechanism of intestinal mucosal IgA responses to commensal bacteria. *Science*. 2000;288(5474):2222–2226.
5. Neutra M, et al. Identification and use of protective monoclonal IgA antibodies against viral and bacterial pathogens. *Adv Exp Med Biol*. 1991;310:179–182.
6. Michetti P, Mahan MJ, Slauch JM, Mekalanos JJ, Neutra MR. Monoclonal secretory immunoglobulin A protects mice against oral challenge with the invasive pathogen Salmonella typhimurium. *Infect Immun*. 1992;60(5):1786–1792.
7. Fagarasan S, Muramatsu M, Suzuki K, Nagaoka H, Hiai H, Honjo T. Critical roles of activation-induced cytidine deaminase in the homeostasis of gut flora. *Science*. 2002;298(5597):1424–1427.
8. Suzuki K, et al. Aberrant expansion of segmented filamentous bacteria in IgA-deficient gut. *Proc Natl Acad Sci U S A*. 2004;101(7):1981–1986.
9. Boullier S, et al. Secretory IgA-mediated neutralization of Shigella flexneri prevents intestinal tissue destruction by down-regulating inflammatory circuits. *J Immunol*. 2009;183(9):5879–5885.
10. Kaetzel CS, Robinson JK, Chintalacharuvu KR, Vaerman JP, Lamm ME. The polymeric immunoglobulin receptor (secretory component) mediates transport of immune complexes across epithelial cells: a local defense function for IgA. *Proc Natl Acad Sci U S A*. 1991;88(19):8796–8800.
11. Burns JW, Siadat-Pajouh M, Krishnaney AA, Greenberg HB. Protective effect of rotavirus VP6-specific IgA monoclonal antibodies that lack neutralizing activity. *Science*. 1996;272(5258):104–107.
12. Kadaoui KA, Corthesy B. Secretory IgA mediates bacterial translocation to dendritic cells in mouse Peyer's patches with restriction to mucosal compartment. *J Immunol*. 2007;179(11):7751–7757.
13. Phalipon A, Cardona A, Kraehenbuhl JP, Edelman L, Sansonetti PJ, Corthésy B. Secretory component: a new role in secretory IgA-mediated immune exclusion in vivo. *Immunity*. 2002;17(1):107–115.
14. Baumann J, Park CG, Mantis NJ. Recognition of secretory IgA by DC-SIGN: Implications for immune surveillance in the intestine. *Immunol Lett*. 2010;131(1):59–66.
15. Peterson DA, McNulty NP, Guruge JL, Gordon JI. IgA response to symbiotic bacteria as a mediator of gut homeostasis. *Cell Host Microbe*. 2007;2(5):328–339.
16. Baklien K, Brandtzaeg P. Immunohistochemical characterization of local immunoglobulin formation in Crohn's disease of the ileum. *Scand J Gastroenterol*. 1976;11(5):447–457.
17. Macpherson A, Khoo UY, Forgacs I, Philpott-Howard J, Bjarnason I. Mucosal antibodies in inflammatory bowel disease are directed against intestinal bacteria. *Gut*. 1996;38(3):365–375.
18. Bouvet JP, Fischetti VA. Diversity of antibody-medi-

ated immunity at the mucosal barrier. *Infect Immun*. 1999;67(6):2687–2691.
19. Talham GL, Jiang HQ, Bos NA, Cebra JJ. Segmented filamentous bacteria are potent stimuli of a physiologically normal state of the murine gut mucosal immune system. *Infect Immun*. 1999; 67(4):1992–2000.
20. Bos NA, et al. Monoclonal immunoglobulin A derived from peritoneal B cells is encoded by both germ line and somatically mutated VH genes and is reactive with commensal bacteria. *Infect Immun*. 1996;64(2):616–623.
21. Quan CP, Berneman A, Pires R, Avrameas S, Bouvet JP. Natural polyreactive secretory immunoglobulin A autoantibodies as a possible barrier to infection in humans. *Infect Immun*. 1997;65(10):3997–4004.
22. Kett K, Baklien K, Bakken A, Kral JG, Fausa O, Brandtzaeg P. Intestinal B-cell isotype response in relation to local bacterial load: evidence for immunoglobulin A subclass adaptation. *Gastroenterology*. 1995;109(3):819–825.
23. Wardemann H, Yurasov S, Schaefer A, Young JW, Meffre E, Nussenzweig MC. Predominant autoantibody production by early human B cell precursors. *Science*. 2003;301(5638):1374–1377.
24. Tiller T, Meffre E, Yurasov S, Tsuiji M, Nussenzweig MC, Wardemann H. Efficient generation of monoclonal antibodies from single human B cells by single cell RT-PCR and expression vector cloning. *J Immunol Methods*. 2008;329(1–2):112–124.
25. Peterson DA, Frank DN, Pace NR, Gordon JI. Metagenomic approaches for defining the pathogenesis of inflammatory bowel diseases. *Cell Host Microbe*. 2008;3(6):417–427.
26. Dunn-Walters DK, Isaacson PG, Spencer J. Sequence analysis of human IgVH genes indicates that ileal lamina propria plasma cells are derived from Peyer's patches. *Eur J Immunol*. 1997;27(2):463–467.
27. Dunn-Walters DK, Boursier L, Spencer J. Hypermutation, diversity and dissemination of human intestinal lamina propria plasma cells. *Eur J Immunol*. 1997;27(11):2959–2964.
28. Yuvaraj S, et al. Evidence for local expansion of IgA plasma cell precursors in human ileum. *J Immunol*. 2009;183(8):4871–4878.
29. Bjerke K, Brandtzaeg P. Terminally differentiated human intestinal B cells. IgA and IgG subclass-producing immunocytes in the distal ileum, including Peyer's patches, compared with lymph nodes and palatine tonsils. *Scand J Immunol*. 1990;32(2):61–67.
30. Fischer M, Kuppers R. Human IgA- and IgM-secreting intestinal plasma cells carry heavily mutated VH region genes. *Eur J Immunol*. 1998;28(9):2971–2977.
31. Tsuiji M, Yurasov S, Velinzon K, Thomas S, Nussenzweig MC, Wardemann H. A checkpoint for autoreactivity in human IgM+ memory B cell development. *J Exp Med*. 2006;203(2):393–400.
32. Tiller T, Tsuiji M, Yurasov S, Velinzon K, Nussenzweig MC, Wardemann H. Autoreactivity in human IgG(+) memory B cells. *Immunity*. 2007; 26(2):205–213.
33. Macpherson AJ, Uhr T. Induction of protective IgA by intestinal dendritic cells carrying commensal bacteria. *Science*. 2004;303(5664):1662–1665.
34. Wijburg OL, Uren TK, Simpfendorfer K, Johansen FE, Brandtzaeg P, Strugnell RA. Innate secretory antibodies protect against natural Salmonella typhimurium infection. *J Exp Med*. 2006;203(1):21–26.
35. Oppezzo P, et al. Somatic mutations can lead to a loss of superantigenic and polyreactive binding. *Eur J Immunol*. 2004;34(5):1423–1432.
36. Haynes BF, et al. Cardiolipin polyspecific autoreactivity in two broadly neutralizing HIV-1 antibodies. *Science*. 2005;308(5730):1906–1908.
37. Witsch EJ, Cao H, Fukuyama H, Weigert M. Light chain editing generates polyreactive antibodies in chronic graft-versus-host reaction. *J Exp Med*. 2006;203(7):1761–1772.
38. Diskin R, Marcovecchio PM, Bjorkman PJ. Structure of a clade C HIV-1 gp120 bound to CD4 and CD4-induced antibody reveals anti-CD4 polyreactivity. *Nat Struct Mol Biol*. 2010;17(5):608–613.
39. Qin J, et al. A human gut microbial gene catalogue established by metagenomic sequencing. *Nature*. 2010;464(7285):59–65.
40. Kabat EA, Wu TT, Perry HM, Gotteman KS, Foeller C. *Sequences Of Proteins Of Immunological Interest*. Vol. 1. 5th ed. Bethesda, Maryland, USA: NIH; 1991.
41. Meffre E, Schaefer A, Wardemann H, Wilson P, Davis E, Nussenzweig MC. Surrogate light chain expressing human peripheral B cells produce self-reactive antibodies. *J Exp Med*. 2004;199(1):145–150.
42. Gonzalez AM, et al. Rotavirus-specific B cells induced by recent infection in adults and children predominantly express the intestinal homing receptor alpha4beta7. *Virology*. 2003;305(1):93–105.